



Predicting Compression Strength of Reinforced Concrete Columns Confined by FRP Using Meta-Heuristic Methods

Mohammadizadeh, M.R.^{1*} and Esfandnia, F.²

¹ Associate Professor, Department of Civil Engineering, University of Hormozgan, Bandar Abbas, Iran.

² Ph.D. Candidate, Department of Civil Engineering, University of Hormozgan, Bandar Abbas, Iran.

© University of Tehran 2021

Received: 10 Jun. 2020;

Revised: 16 May 2021;

Accepted: 25 May 2021

ABSTRACT: There are several methods to predict the compression strength of reinforced concrete columns confined by FRP, such as experimental methods, theory of elasticity and plasticity. Meanwhile, due to its good potential and high accuracy in predicting different problems, the soft computing techniques has attracted considerable attentions. Soft computing includes methods and programs to deal with complex computational problems. The objective of this study is to evaluate and compare the performance of four methods of Least Squares Support Vector Machine (LS-SVM), the Weight Least Squares Support Vector Machine (WLS-SVM), Adaptive Neuro-Fuzzy Inference System (ANFIS) and Particle Swarm Optimization - Adaptive Network based Fuzzy Inference System (PSO-ANFIS) for predicting the compression strength of reinforced concrete columns confined by FRP. A total of 95 laboratory data are selected for use in these methods. The Root Mean Square Error (RMSE) and the correlation coefficient of the results are used to validate and compare the performance of the methods. The results of the study show that the PSO-ANFIS method with the RMSE of 4.610 and the coefficient of determination of $R^2 = 0.9677$ predicts compression strength of reinforced concrete columns confined by FRP with high accuracy and therefore, it can be a good alternative to time-consuming and costly laboratory methods.

Keywords: ANFIS, Compression Strength, FRP-Confined Columns, LS-SVM, PSO-ANFIS, WLS-SVM.

1. Introduction

There are a variety of methods, such as using prefabricated concrete systems, making steel veneers, or composite sheets made of fiber-reinforced polymers (FRPs) for strengthening of reinforced concrete columns. FRPs are among the most desirable materials for repair due to their

high weight-to-strength ratio, anti-corrosion properties, ease of installation and reasonable price. These materials increase the service life of the structure. In order to ensure that large deformations subjected to pre-damage load, in order to achieve sufficient strength in reinforced concrete columns, these columns require lateral confinement. Therefore, when transversal

* Corresponding author E-mail: mrz_mohammadizadeh@hormozgan.ac.ir

reinforcement in reinforced concrete columns is not sufficient, FRP is used for confinement of the columns externally (Haji et al., 2018). Many laboratory studies have examined the strengthening techniques using FRP, some of which can be mentioned (Galal et al., 2005; Chellapandian et al., 2017; Bengar and Shahmansouri, 2020; Choi et al., 2015; Ribeiro et al., 2018; Zeng et al., 2017). Eid et al. (2017) proposed a model based on analytical methods. Comparison of the obtained results showed that the analytical model presented in this study has a very good adaptation with laboratory results and finite element method.

The soft computing techniques have good remarkable accuracy in estimating the relationships between different parameters. Many studies on soft computing in civil engineering have been used to solve complex problems, such as the works conducted by Kamgar et al. (2020), Kar and Pandit (2020), Nematzadeh et al. (2020), Shahmansouri et al. (2019), Shahmansouri et al. (2020), Yasi and Mohammadizadeh (2018), Chou et al. (2019), Kazemi Elaki et al. (2016), Nir et al. (2019) and Taban et al. (2021). Khatibinia and Mohammadizadeh (2017) presented a model for determining the bonding of FRP polymer fibers and building elements. This model was based on ANFIS simulation, and while confirming the accuracy of the ANFIS method, their results in predicting the bonding of FRP polymer fibers and building elements show that the use of the ANFIS model and meta-heuristic models such as PSO and GA can significantly improve the prediction accuracy.

Azimipour et al. (2020) investigated the compressive strength of self-compacting concretes with a high volume of fly ash using linear and nonlinear algorithms in SVM. The results showed that in the case of considering the appropriate input parameters and a wide range of data to obtain the appropriate kernel performance coefficient, the results of the prediction for SVM-RBF method are more accurate than

other SVM methods. Naderpour et al. (2019) provided a relationship to predict the compression strength of reinforced concrete columns confined by FRP using Artificial Neural Networks (ANN). Cascardi et al. (2017) studied the prediction of the compression strength of reinforced concrete columns confined by FRP in circular columns using ANN. The results of this study showed that ANN can be used to predict the compression strength of reinforced concrete columns confined by FRP.

To predict the compression strength of reinforced concrete columns confined by FRP, two different techniques including FRP reinforcing effect and the simultaneous FRP reinforcing effect are considered. In this study, methods have been developed to predict the compression strength of reinforced concrete columns confinement by FRP and transverse reinforcement. For this purpose, a set of experimental data is used for training and testing in the proposed methods. This database includes 95 specimens of FRP-confined columns obtained from different studies. There are 7 input parameters including column height, compressive strength of concrete core without confinement, FRP modulus of elasticity, cross-sectional area of longitudinal reinforcement, yield stress in longitudinal reinforcements, compressive stress due to FRP and shear reinforcement. Here, to estimate the stable stress in the FRP-reinforced columns by soft computational techniques such as Least Squares Support Vector Machine (LS-SVM) method, Weight Least Squares Support Vector Machine (WLS-SVM) and so on, Adaptive Network based Fuzzy Inference System (PSO-ANFIS) are used. Finally, the results of the proposed methods are compared with other available methods.

2. Confinement Stress of FRP Wrap

As the axial pressure is applied to a confined concrete column, the concrete core expands. This expansion and increase in

lateral volume is limited by the surrounding wrap. Therefore, a kind of passive lateral pressure is applied to the middle concrete by the wrap, which is called the confining compressive stress. The distribution of confining compressive stresses in circular sections is quite uniform. Considering the equilibrium of the stresses applied on the repellent material and also regardless of the tangential stresses along the longitudinal direction of the column sample, it can be written that (Purba and Mufti, 1999):

$$f_{lf} = \frac{2 \times t_f \times f_{yf}}{D}, f_{ls} = \frac{2 \times A_{st} \times f_{ys}}{s \times d_c} \quad (1)$$

where D and d_c : are the diameter of column and the diameter of the core, respectively. f_{lf} and f_{ls} : are the compression strength of reinforced concrete columns confined by FRP and transverse reinforcement, respectively. Also t_f : is the thickness of the FRP wrap, f_{yf} : is the maximum tensile stress of FRP, A_{st} : is the cross-sectional area of the transverse reinforcement, f_{ys} : is the yielding stress of the transverse reinforcement and s : is the distance between the transverse reinforcements. The performance manner of concrete, FRP layer and shear reinforcement have been shown in Figure 1. The maximum tensile stress of FRP has been calculated in Eq. (2).

$$f_{yf} = E_f \varepsilon_f \quad (2)$$

where E_f : is the elastic modulus of the FRP wrap in line with the fibers around the column and ε_f : is the ultimate strain of FRP under tension.

The value of ε_f is determined by the Flat Coupon Tensile Test. Laboratory observations show that at the moment of failure, the measured tensile strain of the wrap is less than the value of ε_f . Lam and Teng (2003) used Eq. (3) to calculate the failure strain in the sample of wrapped cylindrical columns with FRP sheets.

$$\varepsilon_{h,wrap} = k_e \varepsilon_f \quad (3)$$

where $\varepsilon_{h,wrap}$: is the circular failure strain of the FRP wrap. k_e : is also the FRP efficiency factor. The value of this coefficient depends on the type of FRP composite.

According to ACI 440.2R-17 (2017), the maximum normal force (P_n) in an element confined by FRP layer, can be calculated using the following equations for elements non-prestressed by existing steel rebar and steel-tie reinforcement, respectively:

$$\phi P_n = 0.85 \phi [0.85 f'_c (A_g - A_{st}) + f_y A_{st}] \quad (4)$$

$$\phi P_n = 0.8 \phi [0.85 f'_c (A_g - A_{st}) + f_y A_{st}] \quad (5)$$

in which A_g and A_{st} : represent the gross and total area of the longitudinal reinforcement, respectively. f_y : denotes the steel reinforcement yield strength and f'_c : represents the maximum compressive strength in confined concrete as follows:

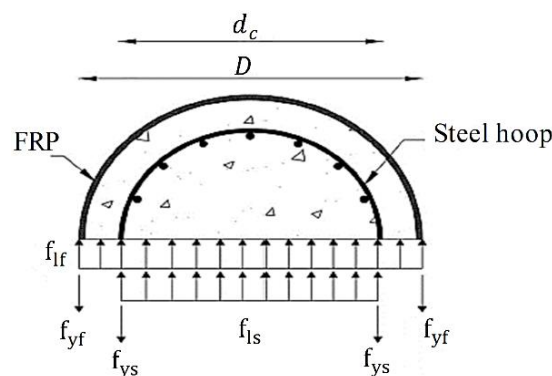


Fig. 1. Mechanism of distribution of concrete stress confined by FRP and transverse reinforcements

$$f'_c = f'_c + \psi_f 3.3k_a f_{lf} \quad (6)$$

in which ψ_f : denotes the reduction factor, which is 0.95, f'_c : represents the compressive strength of unconfined concrete, k_a : is the geometric dependent efficiency factor and f_{lf} : denotes the maximum confinement pressure (Eq. (1)).

3. Laboratory Data

Initially, a laboratory data set consisting of 135 samples (circular columns of reinforced concrete subjected to axial load) was selected (Chastre and Silva, 2010; Demers and Neale, 1999; Benzaid et al., 2010; Matthys et al., 2005; Eid et al., 2009; Abdelrahman and El-Hacha, 2012; Mostofinejad and Torabian, 2015; Silva, 2011; Hadi et al., 2017; Hadi, 2010; Issa et al., 2009; Moshiri et al., 2015; Yin et al., 2015; Hadi, 2006). After collecting the experimental data, the data were excluded to 95 experimental data. Based on Table 1, 12 variables were first gathered from the

references. However, according to the existing algorithms, by calculating the other two parameters using Eq. (1), the number of input parameters was reduced to seven parameters (Table 1). The changes calculated in 95 laboratory data have been shown in Table 2. In order to increase the performance of the LS-SVM, WLS-SVM, ANFIS and PSO-ANFIS methods in the training phase, the values of the input parameters using Eq. (7) are considered in the range [0.1-0.9].

$$S_{I,i} = S_{I,\min} + \left[(S_{I,\max} - S_{I,\min}) \times \frac{D_{I,i} - D_{I,\min}}{D_{I,\max} - D_{I,\min}} \right] \quad (7)$$

where $S_{I,i}$: is the I-th normalized input parameters for the i -th set of parameters in the data. $S_{I,\max}$ and $S_{I,\min}$: are the maximum and minimum values of $S_{I,i}$ for $1 \leq i \leq 95$ the sets of parameter in the data. The values of $D_{I,i}$, $D_{I,\min}$ and $D_{I,\max}$: are the I-th input parameter in the i -th set of the data, minimum and maximum of the data.

Table 1. Description of input and output parameters

Symbol	Parameters
$D(m)$	Concrete section diameter
$L(m)$	Column height
$f'_{co}(MPa)$	Maximum compressive strength of concrete core
$t_f(mm)$	FRP wrap thickness
$E_f(GPa)$	FRP wrap elasticity module
$f_{yf}(MPa)$	Maximum FRP tensile stress
$A_s(mm^2)$	The cross-sectional area of longitudinal reinforcement
$f_y(MPa)$	Yield stress of longitudinal reinforcement
$f_{ys}(MPa)$	Yield stress of transverse reinforcement
$s(m)$	The distance between the transverse reinforcement
$d_b(mm)$	The diameter of the concrete core
$f'_{cu}(MPa)$	Ultimate compressive strength of the columns

Table 2. Statistical description of input and output parameters in the present study

Input parameter	$L(m)$	$f'_{co}(MPa)$	$E_f(GPa)$	$A_{s1}(mm^2)$	$f_y(MPa)$	$f_{yf}(MPa)$	$f_{ys}(MPa)$	$f'_{cu}(MPa)$
Minimum	0.3	25	0	0	0	0	0	26.35
Maximum	2	75	480	2493.8	620	41.8	7.17	164.11
Average	0.95	39.58	102.56	806.53	404.74	11.01	2.38	68.37
Standard deviation	0.45	12.08	87.32	615.36	160.36	9.46	2.11	30.81
Coefficient of variation	0.47	0.3	0.85	0.76	0.4	0.86	0.89	0.45

4. Methods

4.1. Least Squares Support Vector Machine

Strong theoretical evidences show the capability of modeling high non-linear systems based on small sample in Support Vector Machines (SVMs) (Vapnik and Lerner, 1963). The approaches is based on Structural Risk Minimization (SRM) rules (Park and Ang, 1985). Suykens et al. (1999) proposed the Least Squares Support Vector Machine (LS-SVM) to fix the problems of SVM, including the slow training velocity in the large-scale problem.

Consider a set of training data $\{(x_1, y_1) \cdots (x_n, y_n)\} \subset X$, where X implies the input patterns space. The error quadratic norm is considered as the loss function of LS-SVM in the regression modelling of LS-SVM. The optimization problem is expressed as below (Suykens and Vandewalle, 1999):

$$\min J(\omega, \xi) = \frac{1}{2} \omega^2 + \frac{1}{2} C \sum_{i=1}^n \xi_i^2 \quad (8)$$

By considering the equality restriction:

$$y_i = \omega^T \phi(x_i) + b + \xi_i; i = 1, 2, \dots, n \quad (9)$$

Hence, the LS-SVM regression model is defined as below:

$$y(x) = \omega^T \phi(x) + b \quad (10)$$

in Eq. (8), C : denotes the punishment factor to meet tradeoff between the LS-SVM model complexities. The Lagrange function for the optimization problem is:

$$L(\omega, b, \xi_i, \alpha) = \frac{1}{2} \|\omega\|^2 + C \sum_{i=1}^n \xi_i^2 - \sum_{i=1}^n \alpha_i \left[\omega^T \phi(x_i) + b + \xi_i - y_i \right] \quad (11)$$

where $\alpha_i (i=1, 2, \dots, n)$: denotes the Lagrange

multipliers. By eliminating ω and ξ , the Karush–Khun–Tucker (KKT) conditions is:

$$\begin{bmatrix} 0 & 1 & \cdots & 1 \\ 1 & K(x_1, x_1 + \frac{1}{C}) & \cdots & K(x_1, x_n) \\ \vdots & \vdots & \ddots & \vdots \\ 1 & K(x_1, x_n) & \cdots & K(x_n, x_n + \frac{1}{C}) \end{bmatrix} \begin{bmatrix} b \\ \alpha \end{bmatrix} = \begin{bmatrix} 0 \\ y_1 \\ \vdots \\ y_n \end{bmatrix} \quad (12)$$

where $K(.,.)$: represents the so-called kernel function. Based on the Mercer’s condition, a kernel $K(.,.)$ is chosen, such that:

$$K(x, \bar{x}) = \langle \phi(x), \phi(\bar{x}) \rangle_H \quad (13)$$

in fact, the high dimensional feature spaces are described by $K(.,.)$. Therefore, the following LS-SVM model is concluded:

$$y(x) = \sum_{i=1}^n \alpha_i K(x, x_i) + b \quad (14)$$

4.2. Weighted Least Squares-Support Vector Machine

The WLS-SVM regression can be defined as the following optimization in the first weight space by training dataset of N samples $[(x_k, y_k)]_{k=1}^n$ with input data $x_i \in R^d$ and output data $y_i \in R$ (Li et al., 2006):

$$\min J(\omega, \xi_i) = \frac{1}{2} \omega^2 + \frac{1}{2} C \sum_{i=1}^n \bar{v}_i \xi_i^2 \quad (15)$$

$$y_i = \omega^T \phi(x_i) + b + \xi_i; i = 1, 2, \dots, n \quad (16)$$

where $\phi(): R^d \rightarrow R^d$: denotes operator mapping the input into a higher dimensional space; $\omega \in R^d$: is the weight vector in primal weight space; and $\xi_i \in R$ and $b \in R$: are the error variable and bias term, respectively.

The model of WLS-SVM can be formulated by the optimization problem (Eq. (12)) and the training set in the first weight space as follows:

$$y(x) = \omega^T \phi(x) + b \quad (17)$$

In general, the structure of $\phi(x)$ is unknown. So, indirect calculation of ω from Eq. (15) is impossible. Hence, the solutions of WLS-SVM regression will be achieved by constructing a Lagrangian:

$$\begin{aligned} L(\omega, b, e, x) = \\ J(\omega, e) - \sum_{i=1}^n \alpha_i \\ \left[\omega^T \phi(x_i) + b + \xi_i - y_i \right] \end{aligned} \quad (18)$$

where α_i : denotes the Lagrangian multipliers. The optimality is as follows:

$$\frac{\partial L}{\partial \omega} = 0, \frac{\partial L}{\partial b} = 0, \frac{\partial L}{\partial e_i} = 0, \dots, \frac{\partial L}{\partial \alpha_i} = 0 \quad (19)$$

Omitting ω and ξ result the following system:

$$\begin{bmatrix} \Omega + V_\gamma & I_n^T \\ I_n & 0 \end{bmatrix} \begin{bmatrix} a \\ b \end{bmatrix} = \begin{bmatrix} y \\ 0 \end{bmatrix} \quad (20)$$

where

$$V_\gamma = \text{diag} \left\{ \frac{1}{\gamma_1} \dots \frac{1}{\gamma_n} \right\}; \quad (21)$$

$$\Omega_{i,j} = \left\langle \phi(x_i), \phi(x_j) \right\rangle_H;$$

$$i, j = 1, 2, \dots, n$$

$$y = [y_1, \dots, y_n]^T;$$

$$I_n^T = [1, \dots, 1]; \quad (22)$$

$$\alpha = [\alpha_1, \dots, \alpha_n]$$

in which the weight factors \bar{v}_k are given by Widodo and Yang (2008):

$$\bar{v}_k = \begin{cases} 1 & \text{if } \left| \frac{\xi_i}{\hat{\delta}} \right| \leq c_1 \\ \frac{c_2 - \left| \frac{e_i}{\hat{\delta}} \right|}{c_2 - c_1} & \text{if } c_1 \leq \left| \frac{\xi_i}{\hat{\delta}} \right| \leq c_2 \\ 10^{-4} & \text{otherwise} \end{cases} \quad (23)$$

where $\hat{\delta}$: denotes the standard deviation for the error parameters $\xi_i = \frac{d_i}{D_{ij}^{-1}}$; the

constants c_1 and c_2 : are normally selected as $c_1 = 2.5$ and $c_2 = 3$. Here D_{ij}^{-1} : is the i th first diagonal element in D^{-1} , in Eq. (20). According to the Mercer's Theorem, a kernel $K(.,.)$ is:

$$\begin{aligned} K(x_i, \bar{x}_j) = \\ \left\langle \phi(x_i), \phi(\bar{x}_j) \right\rangle_H; \quad (24) \\ i, j = 1, 2, \dots, n \end{aligned}$$

Then, the WLS-SVM model is derived as:

$$y(x) = \sum_{i=1}^n \alpha_i K(x_i, x) + b \quad (25)$$

$K(x_i, \bar{x}_j)$ function is actually a function in the initial space expressed as the inner product of two vectors in the feature space. In order to equate the $K(x_i, \bar{x}_j)$ function with the inner product of two vectors in the feature space, a certain positive $K(x_i, \bar{x}_j)$ function must be symmetric, which holds true in the Mercer condition. The SVM is usually used with three Kernel RBF functions of basic Gaussian radius, polynomials, and the linear Kernel function. The Gaussian radial basis function (RBF) is typically employed as the kernel function in the WLS-SVM approach, which is expressed as:

$$K_{RBF}(x, \bar{x}) = \exp\left(-\frac{\|x - \bar{x}\|^2}{\sigma^2}\right) \quad (26)$$

where σ^2 : denotes a positive real constant, and it is commonly called the kernel width.

4.3. Adaptive Neural Fuzzy Inference System

This system is defined as a neuro-fuzzy that constructs a useful model for different modeling. The structure of ANFIS includes 5 layers (Figure 2):

Layer 1: input for the next layers.

Layer 2: an adaptive step, controlling parameter is calculated based on the membership functions C_j^i in Eq. (27). Two antecedent variables C_i and δ_i for each $\mu C_1^1(x_1)$ are:

$$\mu C_1^1(x_1) = \exp\left(-\frac{(c_i - x)^2}{2\delta_i^2}\right) \quad (27)$$

Layer 3: The calculation of preliminary weights in this layer were done by using

$$w_i = \mu C_1^1(x_1) * \mu C_2^2(x_2) * \dots * \mu C_m^m(x_m) \quad (28)$$

Layer 4: In this layer, the weights calculated from the previous layer are normalized. Eq. (29) shows the normalization of weights.

$$\bar{w}_i = \frac{w_i}{\text{sum}(w_i)} \quad (29)$$

Layer 5: The output of this layer is the total output of the system as shown in Eq. (30). The output value is constructed as sum of f_i and a de-fuzzification step is done to have the final value. ANFIS utilizes the

fuzzy steps as follows:

$$f_i = \bar{w}_i(\alpha_0 + \sum(\alpha_i x_i)) \quad (30)$$

If $x_1 = C_1^k, x_2 = C_2^k, \dots$, and $x_m = C_m^k$, then:

$$f_k = \alpha_0^k + \sum_{i=1}^m \alpha_i^k x_i \quad (31)$$

where x_i : denotes the controlling factors including the column height, compressive strength of concrete core without confinement and FRP modulus of elasticity, C_j^i : represents the linguistic label, $\mu C_j^i(x)$: implies the membership value for determining the dependency of factor (x) to C_{ji} , and α_i : denotes the parameter of linear function for measuring y (Pham et al., 2018).

4.4. Particle Swarm Optimization

Particle Swarm Optimization (PSO) is based on the idea of collective intelligence to find optimal answers in a search space. PSO is formed by a random group of individuals and then optimized by updating generations. In each generation, each person is optimized with two superior positions. The first amount of pbest is the best position that the person has ever reached. The overall best result of Gbest is the other best result that this individual pursues, which represents the optimum location in the entire search of the entire population (Zhou et al., 2011). RMSE is used as the index in this research. By lowering the RMSE, the accuracy of the model will increase.

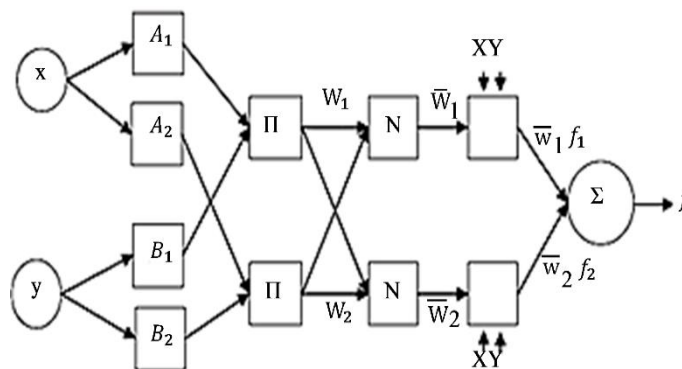


Fig. 2. The structure of the adaptive neural fuzzy inference system (ANFIS)

$$RMSE = \sqrt{\sum_{i=1}^n ((p_i - y_i) / n)} \quad (32)$$

where p_i : denotes the predicted value obtained by the model, y_i : represents the value of the shear strength, and n : implies the number of input data.

The next location will be constructed with the next velocity of a particle if the criteria at position x_i are not met. The formulas are as below:

$$v_i^{k+1} = \omega v_i + ac_1 r_1 (pbest_i - x_i) + ac_2 r_2 (Gbest_i - x_i) \quad (33)$$

$$x_i^{k+1} = x_i + v_i^{k+1} \quad (34)$$

where ω : is the Inertia weight, c_1 and c_2 : are two positive constants known as acceleration coefficients, r_1 and r_2 : are random numbers between 0 and 1, x_i^k : denotes the location of individual i in k , v_i^k : represents the velocity of individual i in k , x_i^{k+1} : implies the location of individual i in $k+1$, v_i^{k+1} : denotes the velocity of individual i in $k+1$, $Pbest$: represents the best location of individual i in the swarm, and $Gbest$: denotes the optimum location of the all individuals in the swarm. The method stops when the criteria are met. Table 3 represents the values of PSO meta-heuristic method. Given the combination of PSO method with ANFIS method for optimization of prior and posterior parameters, the following parameters are selected based on a trial and error process.

Table 3. Parameters related to the PSO method

Number of population	40
Maximum number of iterations	1000
Ideal weight	1
Ideal slope to weight ratio	0.99
Private learning coefficient	1
Public learning coefficient	2

4.5. ANFIS Trained by PSO

The ANFIS method uses the scores related to neural networks and fuzzy systems simultaneously. The main challenge in this method is data training. In ANFIS method, fuzzy anterior and posterior

parameters are adjusted using the gradient descent methods. The responses of the gradient-descent-based method may be stuck in local optimizations. Therefore, the use of meta-heuristic algorithms such as PSO algorithm with random search nature can be considered as alternative and useful approaches. The objective function of the evolutionary algorithms used is the Root Mean Square Error (RMSE). To solve the optimization problem using the PSO-ANFIS algorithms, the w_i weight obtained from the anterior fuzzy parameters and linear parameters are adjusted through meta-heuristic algorithms. Considering the combination of the PSO method with the ANFIS method to optimize the anterior and posterior parameters, the parameters of population size and maximum number of iterations in the PSO algorithm were selected at 40 and 1000, respectively based on a trial and error process. After loading the training data and creating the initial structure, the fuzzy inference system of the Sogeno type was used to train the system designed by PSO and, the training process was repeated 1000 times.

4.6. Performance Indicators

Performance of LS-SVM, WLS-SVM, ANFIS and PSO-ANFIS methods were compared using R^2 , MAPE, MAE and RMSE. The closer the coefficient R^2 are to 1, the closer the predicted values will be to the actual values. Eqs. (35) to (38) show the mathematical formula as the criteria for evaluating performance in the proposed methods in the present study:

$$RMSE = \sqrt{\left[\left(\frac{1}{n} \right) \times \sum_{i=1}^n [p_i - y_i]^2 \right]} \quad (35)$$

$$MAE = \left[\left(\frac{1}{n} \right) \times \sum_{i=1}^n [p_i - y_i] \right] \quad (36)$$

$$MAPE = \left[\left(\frac{1}{n} \right) \sum_{i=1}^n \left[\frac{p_i - y_i}{y_i} \right] \times 100 \right] \quad (37)$$

$$R^2 = \left[\frac{n \sum y_i p_i - (\sum y_i)(\sum p_i)}{\sqrt{((n(\sum y_i^2) - (\sum y_i)^2) \times (n(\sum p_i^2) - (\sum p_i)^2))}} \right]^2 \quad (38)$$

where p_i : is the predicted value and y_i : is the real value for n samples.

5. Discussion

There are simple ways to divid the data. In these methods, the performance of the model is not well demonstrated because of their dependency on which data is selected for training and which data for testing. This dependence sometimes makes the model more accurate and sometimes less accurate. Here, to predict the model, the data were divided into two training and validation classes. The k-fold cross validation method, has been used. To select the k value, it must be ensured that the number of data points in the training subset and the validation subset have a same distribution regime. In this study, 67% of the data were used as a proportion of training subsets and 33% for validation subsets. Using cross-validation k equal to $k = 3$, 59 randomly selected data were used as training and 36 data were used for validation. To predict the compression strength of reinforced concrete columns confined by FRP, the data were trained by four methods of LS-SVM, WLS-SVM, ANFIS and PSO-ANFIS. In the PSO-ANFIS method, a FIS (fuzzy inference system) model was created and PSO is then searches for the most appropriate front and back parameters in ANFIS. To achieve better performance in PSO-ANFIS method, the value of initial parameter of inertia weight is assumed to 1. The RMSE value in this method is also obtained for 1000 iterations. To achieve maximum performance using the LS-SVM and WLS-SVM methods, the most appropriate values for the setting parameter (γ_2) and the RBF core parameter (σ^2) need to be determined. In this study, the best value of monitoring

parameters was determined using trial and error process. Therefore, the setting parameter value (5.1) and the RBF core parameter value (3.09) were selected.

R^2 , MAPE, MAE and RMSE for 95 FRP-confined concrete columns trained by LS-SVM, WLS-SVM, ANFIS and PSO-ANFIS methods are presented in Table 4. According to the coefficients of MAPE, MAE and RMSE, it can be seen that LS-SVM, WLS-SVM, ANFIS and PSO-ANFIS algorithms have generated values close to 1 for the coefficients and values close to zero for the RMSE, MAPE and MAE coefficients. The results also show that the PSO-ANFIS algorithm with $R^2 = 0.984$ in the experimental stage and $R^2 = 0.967$ in the validation stage ($R^2 \geq 0.95$) predicts the parameter with much higher accuracy than the other algorithms. Comparison of the results presented in this table shows that the efficiency and accuracy of the proposed methods to predict the compression strength of reinforced concrete columns confined by FRP is remarkable. The results also show that the PSO-ANFIS method predicts the compression strength of reinforced concrete columns confined by the FRP parameters with much higher accuracy than the other developed methods. Table 5 presents the results of ANN, GMDH, Gene Expression Programming (GEP) and ACI Codes for predicting the compression strength of reinforced concrete columns confined by FRP. Comparison of the results presented in this table with the results obtained from LS-SVM, WLS-SVM, ANFIS and PSO-ANFIS methods shows that the efficiency and accuracy of the proposed methods in the present study to predict the compression strength of reinforced concrete columns confined by FRP is more than the values presented in Codes and other calculation methods.

Table 4. Error measurement in various methods studied in the present study

Methods	LS-SVM		WLS-SVM		PSO -ANFIS		ANFIS	
	Test	Train	Test	Train	Test	Train	Test	Train
Parameter								
MAPE	8.32	6.53	10.72	8.96	11.17	12.58	11.84	12.93
MAE	3.436	3.095	4.140	4.200	3.375	3.060	3.894	1.070
RMSE	6.664	4.163	4.780	4.770	4.610	4.120	4.801	2.078
R^2	0.962	0.980	0.975	0.980	0.967	0.984	0.979	0.995

Table 5. The results of ANN, GMDH, GEP methods and ACI regulations

Method	ANN	GMDH	GEP	ACI
MAPE	5.52	11.49	8.94	34.74
RMSE	5.45	9.93	7.08	33.70
R^2	0.995	0.981	0.991	0.51
Reference	(Naderpour et al., 2019)	(Naderpour et al., 2019)	(Naderpour et al., 2019)	(ACI 440.2R-17, 2002)

The graphs of the ratio of the laboratory data to the predicted data by the training LS-SVM, WLS-SVM, ANFIS and PSO-ANFIS methods are shown in Figures 3-6 respectively. The horizontal axis represents the laboratory data and the vertical axis represents the predicted data. The low scatter of data around the $X = Y$ line indicates a reduction in prediction error and better system performance. Figures 7 to 10 also show the overlap of LS-SVM, WLS-SVM, ANFIS and PSO-ANFIS results with the laboratory data. According to the results of the diagrams, the performance of the PSO-ANFIS method is better than the other methods. The results show that the compressive strength predicted by the PSO-

ANFIS method is well compatible with the compressive strength obtained from the laboratory results. Also, considering all input parameters, PSO-ANFIS method with $RMSE = 4.610$ and $R^2 = 0.967$ has the highest accuracy.

Figure 11 presents the prediction results for all methods used in the present study. The results indicate that four methods of LS-SVM, WLS-SVM, ANFIS and PSO-ANFIS, result a relatively high values of R^2 ($R^2 \geq 0.95$). This shows that these methods have very high accuracy. The compression strength predicted using these methods is also reliable due to the low MAPE coefficient.

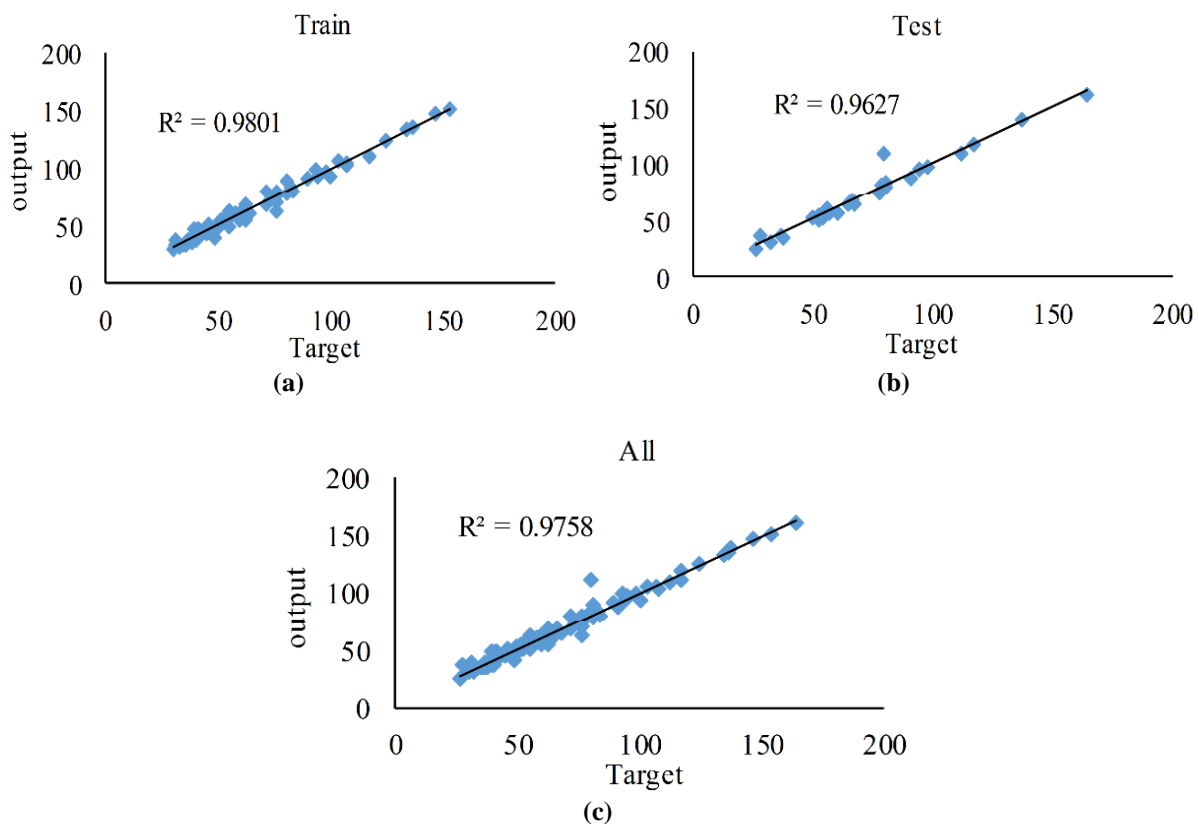


Fig. 3. Comparison of the compression strength predicted in the present study with the values of laboratory compression strength using LS-SVM method: a) Results obtained from the data training phase; b) Results obtained from the data test phase; and c) Results obtained from all laboratory data

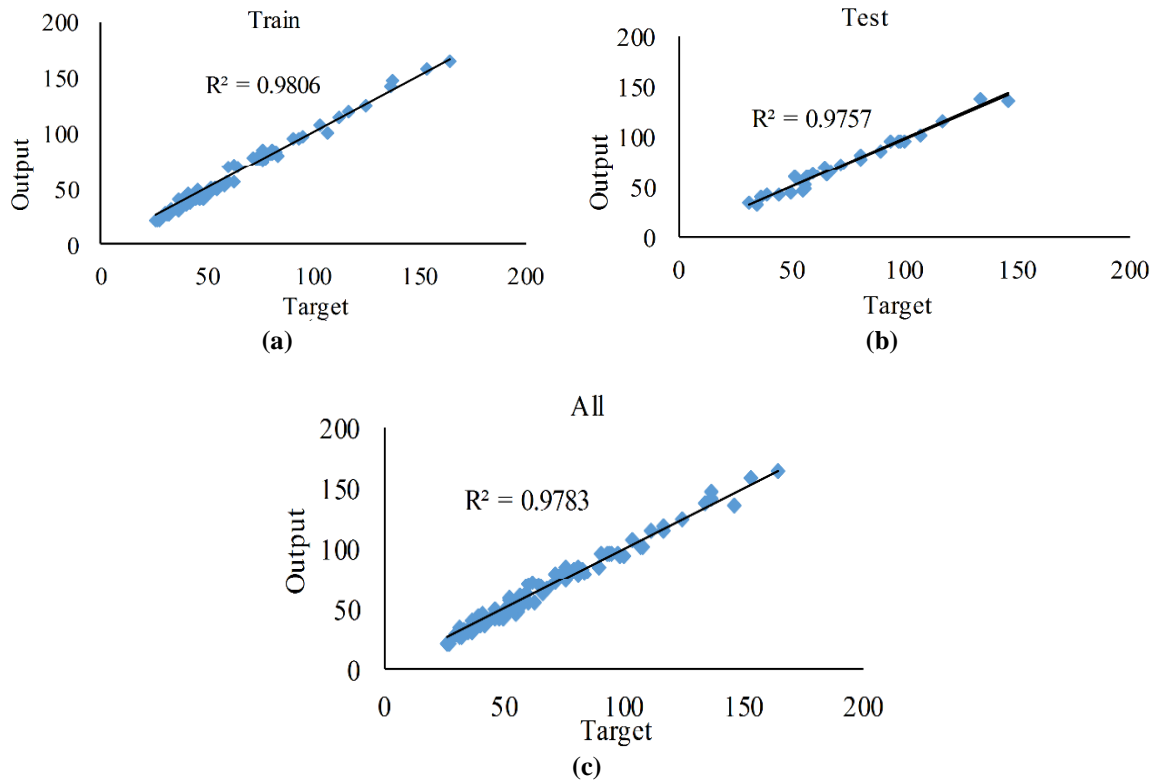


Fig. 4. Comparison of the compression strength predicted in the present study with the values of laboratory compression strength using WLS-SVM method: a) Results obtained from the data training phase; b) Results obtained from the data test phase; and c) Results obtained from all laboratory data

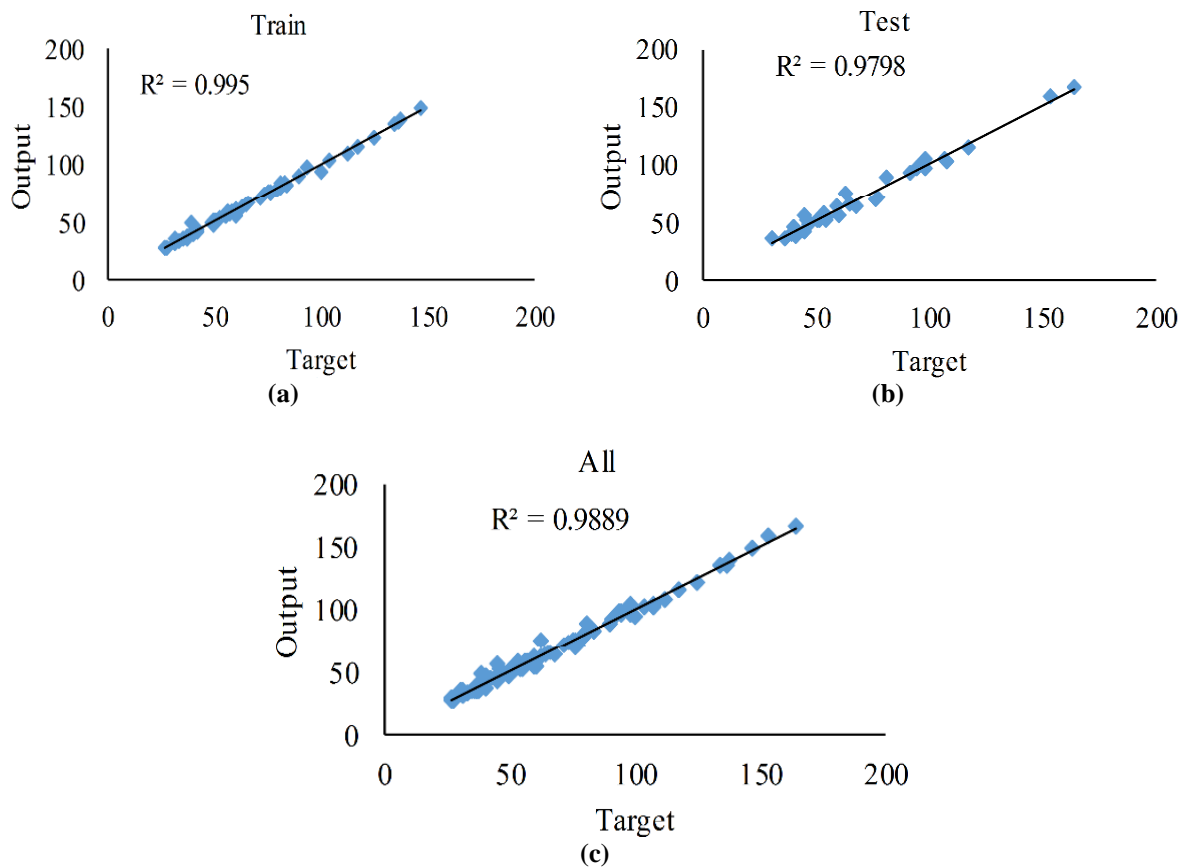


Fig. 5. Comparison of the compression strength predicted in the present study with the values of laboratory compression strength using ANFIS method: a) Results obtained from the data training phase; b) Results obtained from the data test phase; and c) Results obtained from all laboratory data

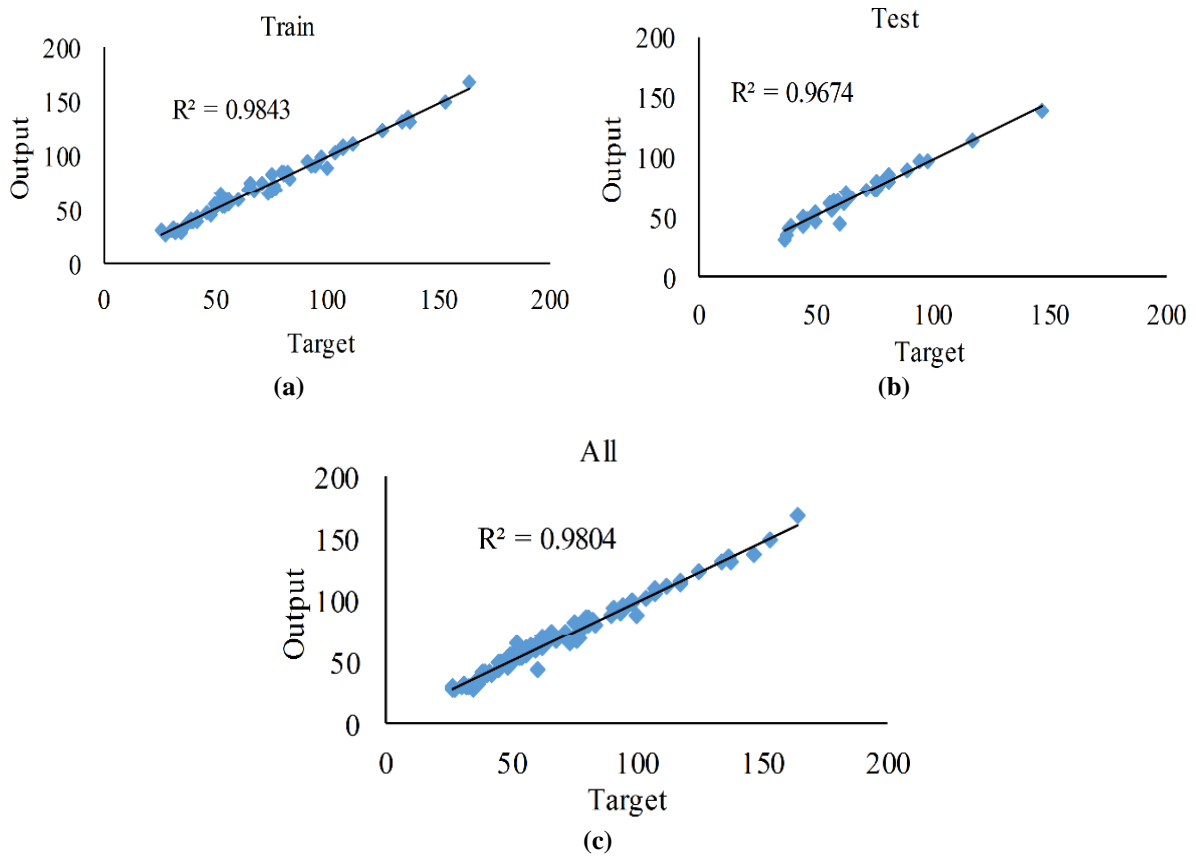


Fig. 6. Comparison of the compression strength predicted in the present study with the values of laboratory compression strength using PSO-ANFIS method: a) Results obtained from the data training phase; b) Results obtained from the data test phase; and c) Results obtained from all laboratory data

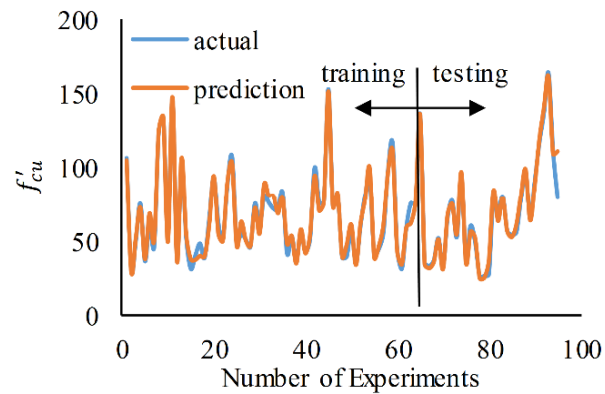


Fig. 7. Comparison of the laboratory results with those predicted by LS-SVM method

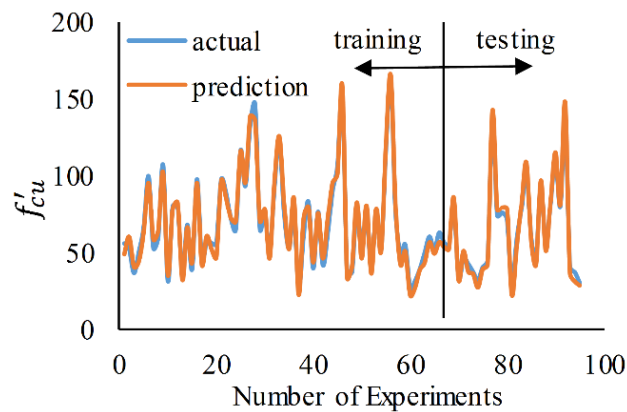


Fig. 8. Comparison of the laboratory results with those predicted by WLS-SVM method

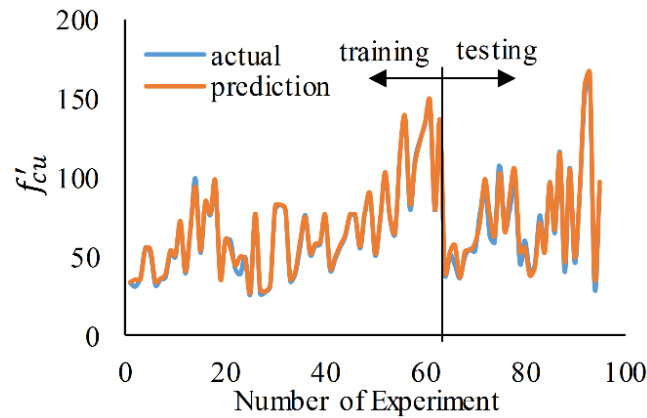


Fig. 9. Comparison of the laboratory results with those predicted by ANFIS method

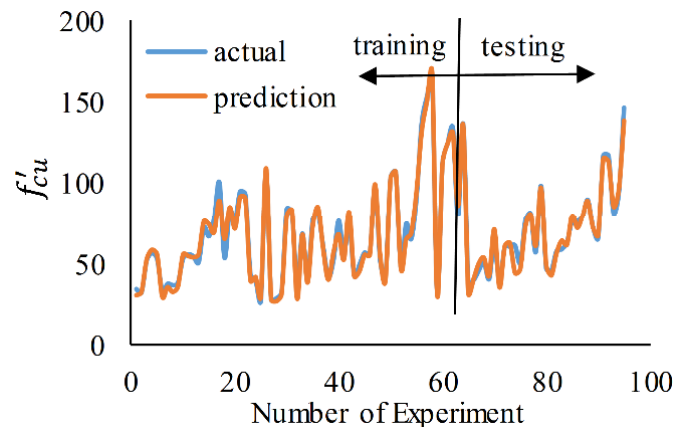


Fig.10. Comparison of the laboratory results with those predicted by PSO-ANFIS method

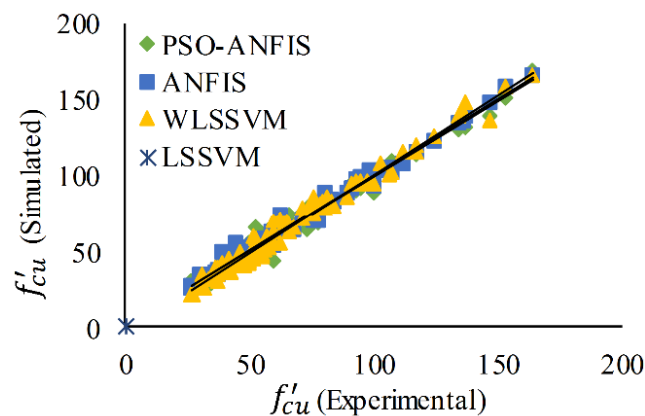


Fig.11. Comparison of the predicted values of compression strength of reinforced concrete columns confined by FRP based on the studied methods in terms of laboratory values

The error of programs code for LS-SVM, WLS-SVM, ANFIS and PSO-ANFIS methods in the training and testing subsets are shown in Figures 12-15 respectively. According to the diagrams, PSO-ANFIS methods have the highest accuracy and the lowest error in predicting the compression strength of reinforced concrete columns confined by FRP. Therefore, this algorithm will be acceptable for designing and

predicting the compression strength of reinforced concrete columns confined by FRP. In addition, despite the minor differences in the performance evaluation values in the training and testing stages, the statistical results show that the methods proposed in this study provide very accurate estimate of the compression strength of reinforced concrete columns confined by FRP.

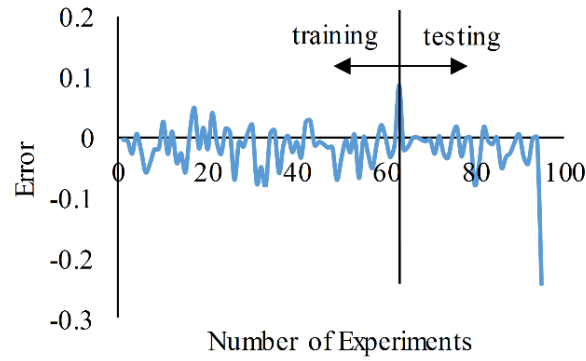


Fig.12. The error values obtained from the LS-SVM method for predicting compression strength of reinforced concrete columns confined by FRP in the training and testing data

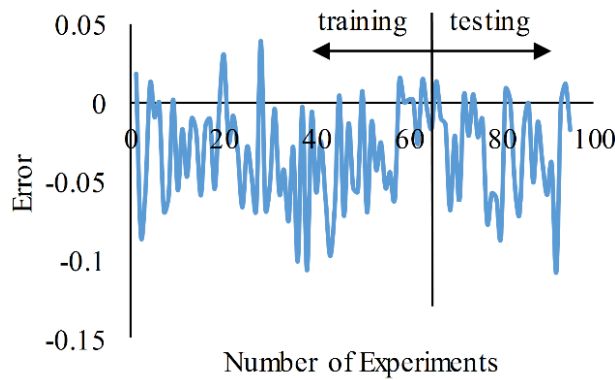


Fig.13. The error values obtained from the WLS-SVM method for predicting compression strength of reinforced concrete columns confined by FRP in the training and testing data

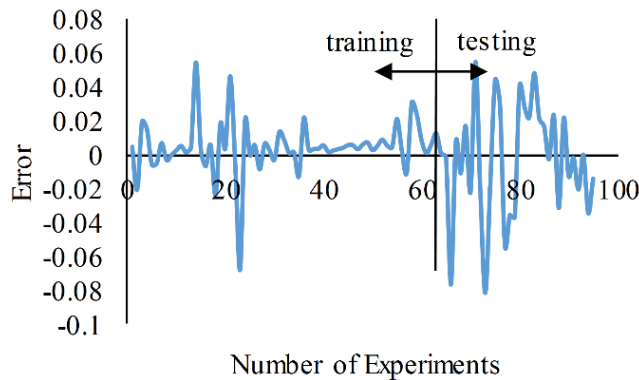


Fig.14. The error values obtained from the ANFIS method for predicting compression strength of reinforced concrete columns confined by FRP in the training and testing data

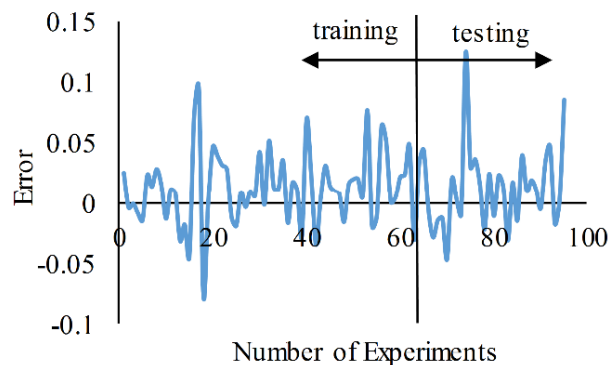


Fig.15. The error values obtained from the PSO-ANFIS method for predicting compression strength of reinforced concrete columns confined by FRP in the training and testing data

6. Conclusions

In this study, the compression strength of reinforced concrete columns confined by FRP was predicted using soft computational methods (LS-SVM, WLS-SVM, ANFIS and PSO-ANFIS). 95 laboratory data were selected for the development of the methods. For the first time, the effect of FRP and shear reinforcement on the strength of the column was also considered simultaneously by seven input parameters. RMSE, R^2 , MAPE and MAE coefficients were calculated for each of the methods and, the outputs of the studied methods were evaluated by other methods. Besides, the error range for each prediction was determined in all methods. Compared to existing models and methods, LS-SVM, WLS-SVM, ANFIS and PSO-ANFIS methods have very good results. The results show that in total the PSO-ANFIS methods with the root mean square error of 4.610 and the coefficient of determination of 0.967 has much accurate prediction than the LS-SVM, WLS-SVM, ANFIS, ANN, GMDH, GEP methods and ACI regulations. Finally, the paper concludes that soft computing is easily applicable to parallel architectures and data processing time with similar results being achieved.

7. References

- Abdelrahman, K. and El-Hacha, R. (2012). "Behavior of large-scale concrete columns wrapped with CFRP and SFRP sheets", *Journal of Composites for Construction*, 16, 430-439.
- ACI 440.2R-17. (2017). "Guide for the design and construction of externally bonded FRP systems for strengthening concrete structures", Reported by ACI committee 440, American Concrete Institute.
- AzimiPour, M., EskandariNaddaf, H. and Pakzad, A. (2020). "Linear and non-linear SVM prediction for fresh properties and compressive strength of high-volume fly ash self-compacting concrete", *Construction and Building Materials*, 230, 117021.
- Bengar, H.A. and Shahmansouri, A.A. (2020). "A new anchorage system for CFRP strips in externally strengthened RC continuous beams", *Journal of Building Engineering*, 30, 101230.
- Benzaid, R., Mesbah, H. and EddineChikh, N. (2010). "FRP-confined concrete cylinders: axial compression experiments and strength model", *Journal of Reinforced Plastics and Composites*, 29(16), 2469-2488.
- Cascardi, A., Micelli, F. and Aiello, M.A. (2017). "An artificial neural networks model for the prediction of the compressive strength of FRP-confined concrete circular columns", *Engineering Structures*, 140, 199-208.
- Chastre, C. and Silva, M.A.G. (2010). "Monotonic axial behavior and modelling of RC circular columns confined with CFRP", *Engineering Structures*, 32, 2268-2277.
- Chellapandian, M., SuriyaPrakash, S. and Sharma, A. (2017). "Strength and ductility of innovative hybrid NSM reinforced and FRP confined short RC columns under axial compression", *Composite Structure*, 176, 205-216.
- Choi, E., Cho, B.S. and Lee, S. (2015). "Seismic retrofit of circular RC columns through using tensioned GFRP wires winding", *Composites Part B Engineering*, 83, 216-225.
- Chou, J.S., Pham, T.P.T., Nguyen T.K., Pham A.D. and Ngo, N.T. (2019). "Shear strength prediction of reinforced concrete beams by baseline, ensemble, and hybrid machine learning models", *Soft Computing*, 24, 3393-3411.
- Demers, M. and Neale, K.W. (1999). "Confinement of reinforced concrete columns with fiber-reinforced composite sheets—an experimental study", *Canadian Journal of Civil Engineering*, 26, 226-241.
- Eid, R. and Paultre, P. (2017). "Plasticity-based model for circular concrete columns confined with fibre-composite sheets", *Engineering Structures*, 29(12), 3301-3311.
- Eid, R., Roy, N. and Paultre, P. (2009). "Normal and high-strength concrete circular elements wrapped with FRP composites", *Journal of Composites for Construction*, 13, 113-124.
- Galal, K., Arafa, A. and Ghobarah, A. (2005). "Retrofit of RC square short columns", *Engineering Structures*, 27(2), 801-813.
- Hadi, M.N.S., Hasan, H.A. and Sheikh, M.N. (2017). "Experimental investigation of circular high strength concrete columns reinforced with glass fiber-reinforced polymer bars and helices under different loading conditions", *Journal of Composites for Construction*, 21(4), 4017005-1-13.
- Hadi, M.N.S. (2010). "Behaviour of reinforced concrete columns wrapped with fibre reinforced polymer under eccentric loads", *Australian Journal of Structural Engineering*, 10(2), 169-178.
- Hadi, M.N.S. (2006). "Comparative study of eccentrically loaded FRP wrapped columns", *Composite Structures*, 74(2), 127-135.
- Haji, M., Naderpour, H. and Kheyroddin, A. (2018). "Experimental study on influence of proposed

- FRP-strengthening techniques on RC circular short columns considering different types of damage index”, *Composite Structures*, 209, 112-28.
- Issa, M.A., Alrousan, R.Z. and Issa, M.A. (2009). “Experimental and parametric study of circular short columns confined with CFRP composites”, *Journal of Composites for Construction*, 13(2), 135-147.
- Kamgar, R., Bagherinejad, M.H. and Heidarzadeh, H. (2020). “A new formulation for prediction of the shear capacity of FRP in strengthened reinforced concrete beams”, *Soft Computing*, 24, 6871-6887.
- Kar, S., Pandit, A.R. and Biswal, K.C. (2020). “Prediction of FRP shear contribution for wrapped shear deficient RC beams using adaptive neuro-fuzzy inference system (ANFIS)”, *Structures*, 23, 702-717.
- Kazemi Elaki, N., Shabakhty, N., Abbasi Kia, M. and Sanayee Moghaddam, S. (2016). “Structural reliability: an assessment using a new and efficient two- phase method based on artificial neural network and a harmony search algorithm”, *Civil Engineering Infrastructures Journal*, 49(1), 1-20.
- Khatibinia, M. and Mohammadzadeh, M.R. (2017). “Intelligent fuzzy inference system approach for modeling of debonding strength in FRP retrofitted masonry elements”, *Structural Engineering and Mechanics*, 56(5), 787-796.
- Lam, L. and Teng, J.G. (2003). “Design-oriented stress-strain model for FRP-confined concrete in rectangular columns”, *Journal of Reinforced Plastics and Composites*, 22(13), 1149-1186.
- Li, H.S., Lü, Z.Z. and Yue, Z.F. (2006). “Support vector machine for structural reliability analysis”, *Applied Mathematics and Mechanics*, 27(10), 1135-1143.
- Matthys, S., Toutanji, H., Audenaert, K. and Taerwe, L. (2005). “Axial load behavior of large-scale columns confined with fiber-reinforced polymer composites”, *ACI Structural Journal*, 102, 258-267.
- Moshiri, N., Hosseini, A. and Mostofinejad, D. (2015). “Strengthening of RC columns by longitudinal CFRP sheets: Effect of strengthening technique”, *Construction and Building Materials*, 79, 318-325.
- Mostofinejad, D. and Torabian, A. (2015). “Experimental study of circular RC columns strengthened with longitudinal CFRP composites under eccentric loading: comparative evaluation of EBR and EBROG methods”, *Journal of Composites for Construction*, 20(2), 4015055-1-15.
- Naderpour, H., Nagai, K., Fakharian, P. and Haji, M. (2019). “Innovative models for prediction of compressive strength of FRP-confined circular reinforced concrete columns using soft computing methods”, *Composite Structures*, 215, 69-84.
- Nair, A., Cai C.S. and Kong X. (2019). “Acoustic emission pattern recognition in CFRP retrofitted RC beams for failure mode identification”, *Composites Part B: Engineering*, 161, 691-701.
- Nematzadeh, M., Shahmansouri, A.A. and Fakoor, M. (2020). “Post-fire compressive strength of recycled PET aggregate concrete reinforced with steel fibers: Optimization and prediction via RSM and GEP”, *Construction and Building Materials*, 252, 119057.
- Park, Y.J. and Ang, A.H.S. (1985). “Mechanistic seismic damage model for reinforced concrete”, *Journal of Structural Engineering*, 111(4), 722-739.
- Pham, B.T., Hoang T.A., Nguyen, D.M. and Bui, D.T. (2018). “Prediction of shear strength of soft soil using machine learning methods”, *Catena*, 166, 181-191.
- Purba, B.K. and Mufti, A.A. (1999). “Investigation of the behavior of circular concrete columns reinforced with carbon fiber reinforced polymer (CFRP) jackets”, *Canadian Journal of Civil Engineering*, 26(5), 590-596.
- Ribeiro, F., Sena-Cruz, J., Branco, F.G. and Júlio, E. (2018). “Hybrid FRP jacketing for enhanced confinement of circular concrete columns in compression”, *Construction and Building Material*, 184, 681-704.
- Shahmansouri, A.A., Akbarzadeh Bengar, H. and Ghanbari, S. (2020). “Compressive strength prediction of eco-efficient GGBS-based geopolymer concrete using GEP method”, *Journal of Building Engineering*, 31, 101326.
- Shahmansouri, A.A., Akbarzadeh Bengar, H. and Jahani, E. (2019). “Predicting compressive strength and electrical resistivity of eco-friendly concrete containing natural zeolite via GEP algorithm”, *Construction and Building Materials*, 229, 116883.
- Silva, M.A.G. (2011). “Behavior of square and circular columns strengthened with aramid or carbon fibers”, *Construction and Building Materials*, 25(8), 3222-3228.
- Suykens, J.A.K., DeBrabanter, J., Lukas, L. and Vandewalle, J. (2002). “Weighted least squares support vector machines: Robustness and sparse approximation”, *Neurocomputing*, 48(1-4), 85-105.
- Suykens, J.A.K. and Vandewalle, J. (1999). “Least squares support vector machine classifiers”, *Neural Processing Letters*, 9(3), 293-300.
- Taban, M.H., Hajiazizi, M., and Ghobadian, R. (2021). “Prediction of Q-value by multi-variable regression and novel Genetic Algorithm based on the most influential parameters”, *Civil Engineering Infrastructures Journal*, 54(2), 267-280.
- Yasi, B. and Mohammadzadeh, M.R. (2018).

- “Identification of structural defects using computer algorithms”, *Civil Engineering Infrastructures Journal*, 51(1), 55-86.
- Yin, P., Huang, L., Yan, L. and Zhu, D. (2015). “Compressive behavior of concrete confined by CFRP and transverse spiral reinforcement. Part A: experimental study”, *Materials and Structures*, 49(3), 1001–1011.
- Zeng, J.J., Guo, Y.C., Gao, W.Y., Li, J.Z. and Xie, J.H. (2017). “Behavior of partially and fully FRP-confined circularized square columns under axial compression”, *Construction and Building Materials*, 152, 319-332.
- Zhou, D., Gao, X., Liu, G., Mei, C., Jiang, D. and Liu, Y. (2011). “Randomization in particle swarm optimization for global search ability”, *Expert Systems with Applications*, 38(12), 15356-15364.



This article is an open-access article distributed under the terms and conditions of the Creative Commons Attribution (CC-BY) license.